Human Apolipoprotein(a) Kringle V Inhibits Ischemia-Induced Retinal Neovascularization via Suppression of Fibronectin-Mediated Angiogenesis

Yangmi Lim,[1] Dong Hyun Jo,[2,3,4] Jin Hyoung Kim,[2] Jin-Hyung Ahn,[1] Yu Kyeong Hwang,[1] Dong-Ku Kang,[5] Soo-Ik Chang,[5] Young Suk Yu,[2,3] Yeup Yoon,[1] and Jeong Hun Kim[2,3,4]

Retinal neovascularization is observed in progression of diabetic retinopathy. New vessels grow into the vitreous cavity in proliferative diabetic retinopathy, resulting in traction retinal detachment and vitreous hemorrhage. To overcome the catastrophic visual loss due to these complications, efforts have been focused on the treatment of retinal neovascularization. In this study, we demonstrated the inhibitory effect of recombinant human apolipoprotein(a) kringle V (rhLK8) in an animal model of ischemia-induced retinal neovascularization. rhLK8 induced no definite toxicity on endothelial cells and retinal tissues at the therapeutic dosage. Interestingly, rhLK8 showed antiangiogenic effect, particularly on fibronectin-mediated migration of endothelial cells. Further experiments demonstrated high binding affinity of rhLK8 to $\alpha3\beta1$ integrin, and suppression of it might be the mechanism of antiangiogenic effect of rhLK8. Furthermore, rhLK8 inhibited phosphorylation of focal adhesion kinase, resulting in suppression of activation of consequent p130CAS-Jun NH_2-terminal kinase. Taken together, our data suggested the possible application of rhLK8 in the treatment of retinal neovascularization by suppression of fibronectin-mediated angiogenesis. *Diabetes* **61:1599–1608, 2012**

R etinal neovascularization from inner layers of the retina is observed in proliferative diabetic retinopathy (DR) (1). New vessels grow into the vitreous cavity, which consists of various extracellular matrix (ECM) proteins, resulting in traction retinal detachment and vitreous hemorrhage (2). As a result of these complications, DR is the leading cause of blindness in working populations (3). Vitreous functions as the scaffold for new vessel ingrowth and interacts with endothelial cells. However, current treatment options for DR, laser photocoagulation, and vitrectomy, have limitations because they do not target interactions between endothelial cells and the vitreous.

Of the ECM proteins in the vitreous, fibronectin (FN) is second to collagen in quantity (4). Especially in patients with DR, FN was increased in the retina, vitreous, and newly formed capillaries (5–8). Furthermore, tight glycemic control downregulated the expression of FN in diabetic rats (9). In this regard, FN-mediated angiogenesis might be a validated target for the treatment of DR.

We previously reported the antiangiogenic effect of recombinant human apolipoprotein(a) kringle V (rhLK8) (10). A cryptic apolipoprotein(a) kringle domain, containing kringle IV-9, IV-10, and V, also suppressed migration of endothelial cells and angiogenesis-dependent tumor growth (11). Interestingly, rhLK8 inhibited fibroblast growth factor (FGF)–stimulated phosphorylation of focal adhesion kinase (FAK), suggesting possible interference of rhLK8 in the interaction between ECM and endothelial cells. In general, the kringle domain mediates functions such as growth factors, proteases, or coagulation factors (10). Moreover, it is a conserved architecture to inhibit blood vessel growth, and disulfide bond-linked kringle structures are vital for the antiangiogenic effect of molecules containing kringle domains, such as angiostatin (12).

In this study, we demonstrated that rhLK8 suppressed retinal neovascularization. Interestingly, rhLK8 inhibited the migration of endothelial cells mediated by FN, not collagen or vitronectin (VN). Furthermore, our results showed high binding affinity of rhLK8 to $\alpha3\beta1$ integrin and downstream inhibition of activation of FAK, p130 Crk-associated substrate (p130CAS), and c-Jun NH_2-terminal kinase (JNK). Taken together, rhLK8 could be a possible inhibitor of retinal neovascularization via suppression of FN-mediated angiogenesis in DR.

RESEARCH DESIGN AND METHODS

Cell culture. Human umbilical vein endothelial cells (HUVECs) were purchased from Lonza (Basel, Switzerland) and maintained in endothelial basal medium-2 (EBM-2) containing bovine brain extract. SNUOT-Rb1 cells from the human retinoblastoma cell line established by our group (13) were maintained in RPMI 1640 medium (WelGENE, Daegu, Korea), supplemented with 10% FBS (Gibco BRL, Rockville, MD). Cells were cultured at 37°C in a moist atmosphere of 95% air and 5% CO_2.

Animals. C57BL/6 mice were purchased from Samtako (Seoul, Korea) and were kept in alternate 12 h dark/light cycles at room temperature (RT). Care, use, and treatment of animals were done in agreement with the Association for Research in Vision and Ophthalmology for the use of animals in ophthalmic and vision research.

Antibodies. Antibodies to paxillin and p130CAS were obtained from Upstate Biotechnology (Billerica, MA). Texas red-conjugated phalloidin was purchased from Invitrogen (Carlsbad, CA). Antibodies to integrin $\beta1$, $\beta3$, αv, $\alpha3$, and $\alpha5$ were obtained from Chemicon (Billerica, MA). Antibodies against rhLK8 were purified from ascites fluid of mice that were implanted with hybridoma cells producing monoclonal antibodies against rhLK8 (Adipogen Inc., Incheon, Korea). Rabbit anti-phospho–stress-activated protein kinase (SAPK)/JNK, anti-SAPK/JNK, anti-phospho–p44/42 MAP kinase, antip44/42 MAP kinase, anti-FAK,

and anti-phospho–FAK were obtained from Cell Signaling Technology (Danvers, MA).

Preparation of rhLK8. The *Saccharomyces cerevisiae* BJ3501 strain was transformed using an expression vector for rhLK8, which was constructed to express rhLK8 fused to the α factor signal sequence under the control of the yeast Gal1 promoter, followed by processing that allows its secretion into the culture medium (14). The rhLK8 protein was purified to homogeneity from the BJ3501 culture supernatant, as previously described (15).

Cell viability assay. HUVECs and SNUOT-Rb1 cells were treated with rhLK8 for 24 h. The medium was replaced with fresh medium containing 0.5 mg/mL 3-(4,5-dimethylthiazol-2-yl)-2,5-diphenyltetrazolium bromide (MTT). The medium was removed after 4 h, and the resultant purple formazan product was suspended with DMSO. The absorbance of the solution was measured at 560 nm using a microplate reader (Molecular Devices, Sunnyvale, CA).

Histologic analysis and transferase-mediated dUTP nick-end labeling (TUNEL) assay. We intravitreally injected 10 μmol/L rhLK8 into the right eye of 8-week-old female C57BL/6 mice. We chose this concentration as the maximal therapeutic dosage. The mice were killed after 1 week, and for histologic analysis, hematoxylin and eosin staining was performed on the enucleated eye. Retinal thickness and the presence of inflammatory cells were assessed. TUNEL was done with the TUNEL fluorescein kit (Roche, Basel, Switzerland). TUNEL-positive cells were counted with a fluorescence microscope (Olympus, Tokyo, Japan).

Oxygen-induced retinopathy (OIR) mice. We induced OIR in mice as previously described (16), modified from the original protocol by Smith et al. (17). Briefly, at postnatal day (P) 7, mice were exposed to hyperoxia (75 ± 0.5% O_2) for 5 days and then returned to room air. To assess the antiangiogenic effect of rhLK8, we intravitreally injected rhLK8 at P14. For quantitative analysis of retinal neovascularization, we counted the vascular lumens on the vitreal side of the inner limiting membrane from each eye at P17.

Tube formation assay. Tube formation assay was performed as we previously described (18). HUVECs were placed on the Matrigel and treated with rhLK8 or vascular endothelial growth factor (VEGF; Sigma-Aldrich, St. Louis, MO) for 12 h. Tube formation was quantified by counting the number of connected cells in randomly selected fields and dividing by the total number of cells in the same field.

Wound migration assay. Cell migration was assessed with wound migration assay as we previously described (19). HUVECs were placed on the gelatin-treated culture dishes and were wounded with a blade. After treatment with rhLK8 or VEGF (Sigma-Aldrich) for 12 h, the degree of migration was quantified by counting the cells that migrated beyond the reference line.

Migration assay. Boyden chambers (Corning, Corning, CA) were coated with VN, collagen, or FN for 2 h at RT. Membranes were washed with PBS and air dried for 2 h. The cells were treated with rhLK8, antibodies against several subtypes of integrins or inhibitors, such as SP600125 (Calbiochem, Darmstadt, Germany), LY204002 (Calbiochem), and U0126 (Calbiochem), for 30 min in suspension. The cells were added to each Boyden chamber and incubated for 4 h at 37°C. After the incubation, cells were fixed and stained with crystal violet. The degree of migration was determined by measuring the absorbance of eluted dye solution at 595 nm.

Cell adhesion assay. HUVECs were treated with 0.5% BSA or rhLK8 for 30 min in suspension. Then, the cells were inoculated onto the plate coated with VN, collagen, or FN (10 μg/mL) in the absence of serum. Phase-contrast images were used to analyze cell adhesion to ECM proteins.

Immunofluorescent staining. HUVECs were plated onto the coverslips coated with VN, collagen, or FN (10 μg/mL) and incubated for 90 min. Then, the cells were pretreated with antibodies to α and β subunits of integrin (2 μg/mL), or rhLK8 (1 μmol/L) for 60 min, fixed in 4% paraformaldehyde for 10 min, permeabilized with 0.05% Triton-X100 for 5 min, and blocked with 0.05% BSA for 1 h at RT. Cells were immunolabeled with primary antibody against paxillin, integrin β1, or rhLK8 overnight at 4°C. Coverslips were incubated with fluorescein-conjugated secondary antibodies or Texas red-conjugated phalloidin and mounted with mounting medium (Vectashield, Vector Laboratories, Burlingame, CA). Cells were examined via a fluorescence microscope (Model Axiophot-2, Carl Zeiss).

Flow cytometry. HUVECs were stained with fluorescein isothiocyanate–conjugated mouse anti-human monoclonal antibodies to integrin β1, β3, αv, α3, and α5, and analyzed with the FACSCalibur apparatus (BD Immunocytometry Systems, San Jose, CA).

Protein microarray. We performed protein microarray using ProteoChip (Proteogen, Chuncheon, Korea) (20). Mixtures of antibodies to integrin α subunits and integrin β subunits were immobilized on the ProLinker-coated microarray spot surface. Integrin subunits (integrin αv, α1, α3, α5, β1, β3; Abcam, Cambridge, U.K.) were immobilized on the antibodies to integrins for 1 h at RT. The microarray was incubated with Cy3-labeled rhLK8 for 1 h at 23°C and scanned using a fluorescence scanner (Molecular Devices).

Small interfering (si)RNA transfection. siRNAs for integrin β1 and β3 were purchased from Dharmacon (Lafayette, CO). The control sequences were fluorescent oligonucleotides that localized to the nucleus (Dharmacon). Transfection was performed with DharmaFECT reagent (Dharmacon) according to the manufacturer's instructions. Briefly, HUVECs were transfected with a mixture of 2 μL DharmaFECT reagent and 4 μg siRNA. After 24 h, the medium was replaced with medium containing 10% FBS. After 48 h, the cells were prepared for immunoblotting or migration assay.

Immunoprecipitation and immunoblotting. The cells were lysed in radio-immunoprecipitation assay buffer containing protease inhibitors. The lysates were clarified by centrifugation at 10,000*g* for 15 min at 4°C, denatured with SDS buffer, boiled, and analyzed by SDS-PAGE. For immunoprecipitation, each sample was incubated with the relevant antibody for 2 h at 4°C and then with protein G-Sepharose beads for 1 h. Immune complexes were collected by centrifugation. For immunoblotting, the proteins were transferred onto polyvinylidene difluoride membranes (GE Healthcare, Cardiff, U.K.), which were incubated with appropriate primary antibodies, followed by species-specific horseradish peroxidase–conjugated secondary antibodies (GE Healthcare). The membranes were treated with Amersham ECL Western blotting detection reagent (GE Healthcare) and exposed to the film (Amersham Hyperfilm ECL, GE Healthcare).

Statistics. Values between groups were compared with the Mann-Whitney *U* test, and analyses were performed using SPSS 12.0 software (SPSS, Chicago, IL). Mean ± standard deviation was shown. Values of $P < 0.05$ were considered statistically significant.

RESULTS

rhLK8 inhibits retinal neovascularization without toxicity. To investigate whether rhLK8 induced cellular toxicity, we performed MTT assay on HUVECs and SNUOT-Rb1 cells. At concentrations of 0.1 to 10 μmol/L, rhLK8 did not affect the viability of both cells (Fig. 1*A* and *B*). The injection of 10 μmol/L intravitreally into eyes of C57BL/6 mice, induced no change in structural integrity, inflammation, or apoptosis (Fig. 1*C*).

We previously reported the antiangiogenic effect of rhLK8 with chick chorioallantoic membrane and Matrigel plug assays (10). In this study, as shown in Fig. 1*D*, rhLK8 reduced retinal neovascularization in a dose-dependent manner at the concentrations of 0.1 to 10 μmol/L in the mouse model of OIR.

rhLK8 inhibits angiogenic processes: tube formation and migration of endothelial cells. In the process of angiogenesis, endothelial cells migrate toward surrounding ECM and proliferate to form vascular structures (21). We further investigated antiangiogenic effect of rhLK8 in in vitro angiogenesis assays, tube formation, and wound migration assays. As shown in Fig. 2*A*, rhLK8 reduced the degree of tube formation stimulated by VEGF. We previously reported the inhibitory effect of rhLK8 on FGF-mediated endothelial migration (10). In this study, rhLK8 also suppressed migration of HUVECs stimulated by VEGF (Fig. 2*B*). From these results, we concluded that the in vivo antiangiogenic effect of rhLK8 might be due to the suppression of angiogenesis processes.

rhLK8 suppresses migration of endothelial cells on FN and FN-stimulated formation of actin stress fibers and focal adhesions. We previously reported that rhLK8 did not affect phosphorylation of extracellular signal–related kinase (ERK) 1/2 and Akt, but reduced phosphorylation of FAK (10). From these results, the action of rhLK8 was thought to be interference with cell–ECM interaction. To verify this hypothesis, we investigated the effect of rhLK8 on the migration of HUVECs according to ECM proteins and found rhLK8 only affected migration via Boyden chambers precoated with FN (Fig. 3*A*).

To determine the effect of rhLK8 on the adhesion between ECM and endothelial cells, we evaluated morphologic changes of endothelial cells on ECM proteins. Phase-contrast
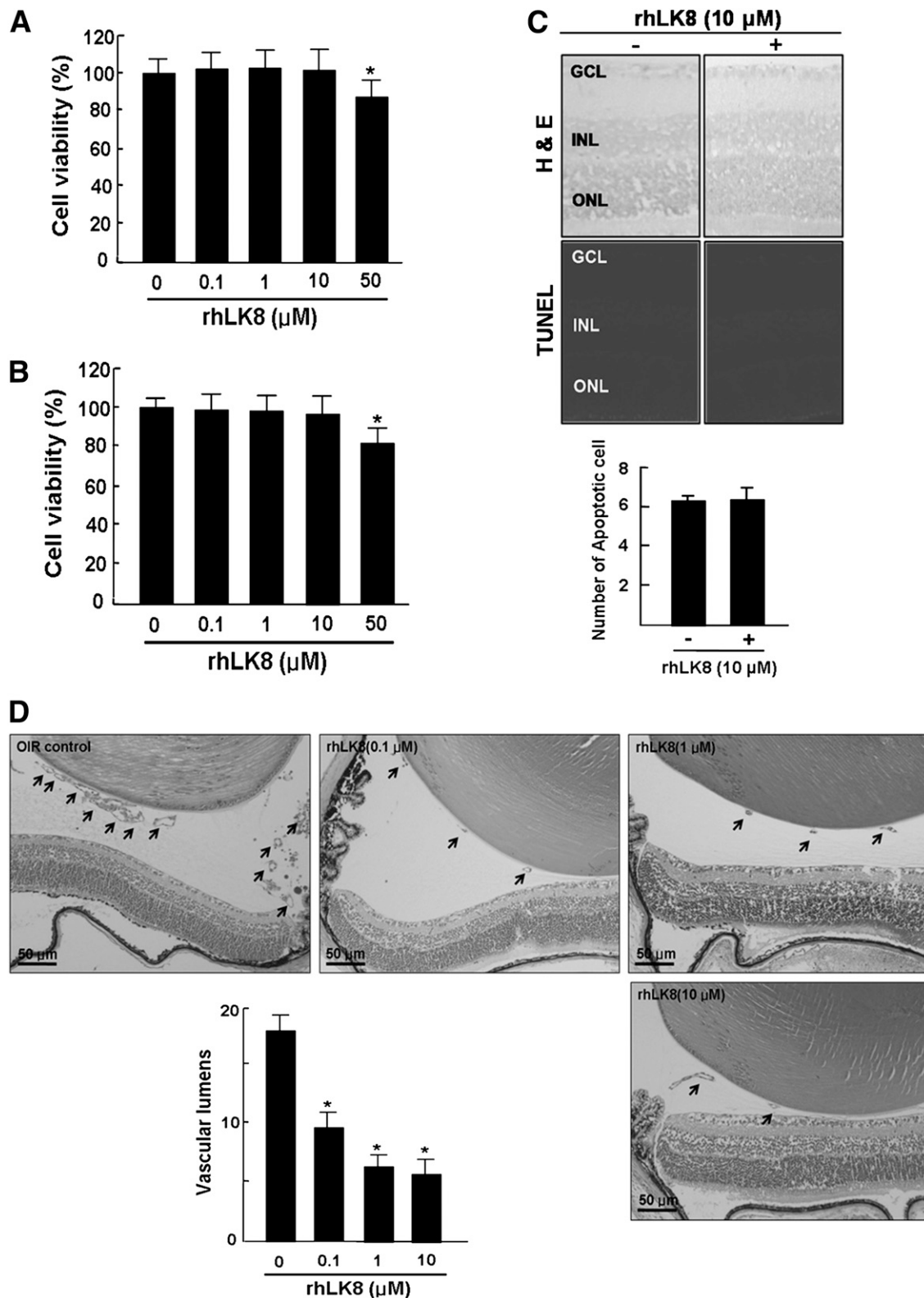
FIG. 1. rhLK8 inhibits retinal neovascularization in a dose-dependent manner without cellular or retinal toxicity. rhLK8 did not induce a decrease in the viability of HUVECs (A) and SNUOT-Rb1 cells (B) at the concentration of between 0.1 and 10 μmol/L. C: There was no increase in in-flammatory and apoptotic cells in the retina when rhLK8 was injected intravitreally at the concentration of 10 μmol/L. GCL, ganglion cell layer; INL, inner nuclear layer; ONL, outer nuclear layer. D: A mouse model of OIR was used to determine the inhibitory effect of rhLK8 on retinal neovascularization. Newborn mice were exposed to hyperoxia for 5 days (from P7 to P11) and then returned to room air for another 5 days. Retinal neovascularization peaks at P17. We intravitreally injected rhLK8 (0.1–10 μmol/L in 1 μL PBS) at P14. Quantitative analysis was performed by counting the vascular lumens (arrows) on the vitreal side of the inner limiting membrane in 10 sections from each eye. The average lumens per section for each group are presented as mean ± SD. *$P < 0.05$.
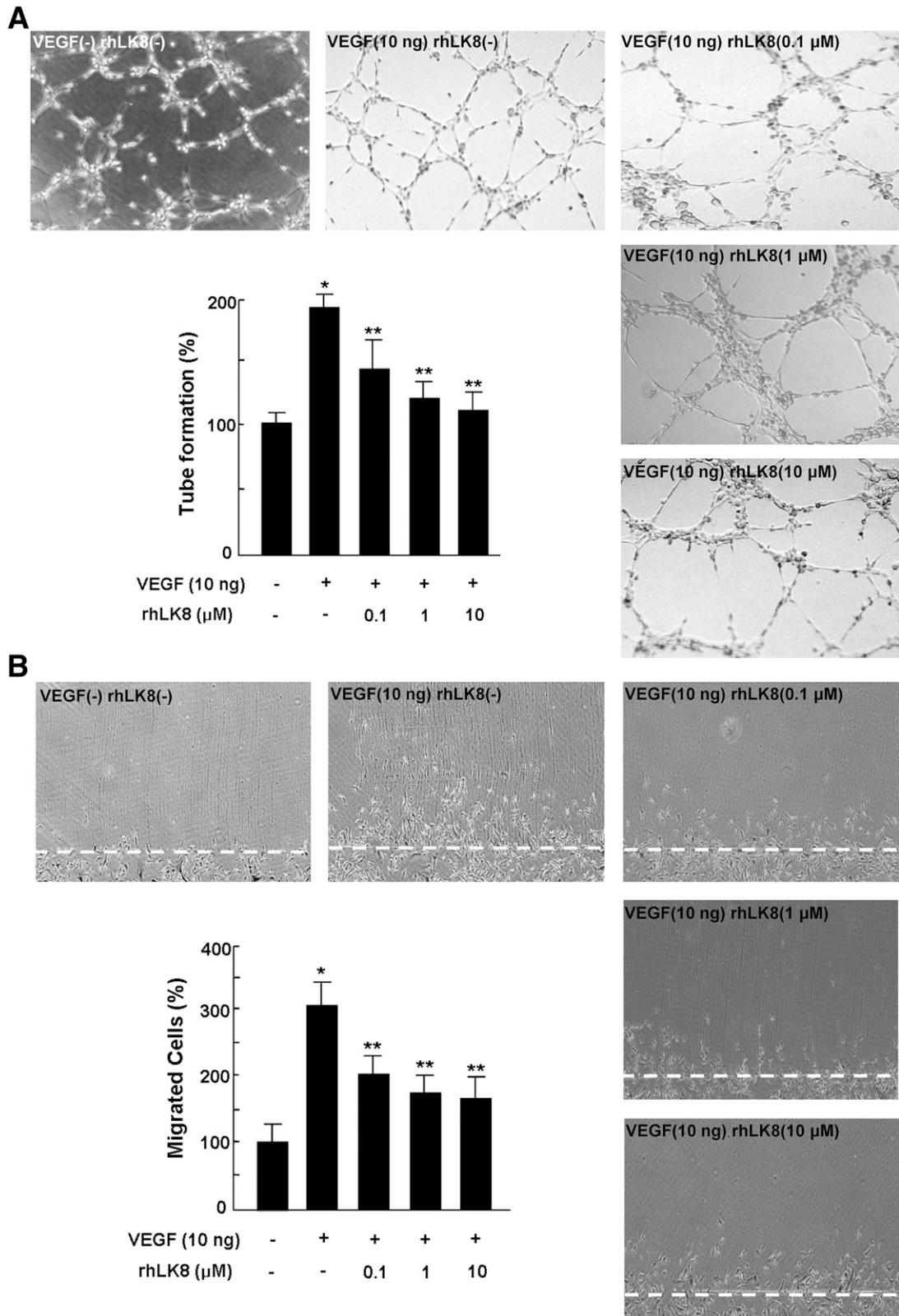
FIG. 2. rhLK8 inhibits in vitro tube formation and migration of endothelial cells. We performed in vitro angiogenesis assays, tube formation, and wound migration assays to investigate the inhibitory effect of rhLK8 on the process of angiogenesis. *A*: Tube formation was quantified by counting the number of connected cells in randomly selected fields (original magnification ×200) via the light microscope and dividing the number by the total number of cells in each field. rhLK8 effectively reduced the degree of tube formation stimulated by VEGF in a dose-dependent manner. *B*: To assess the inhibitory effect of rhLK8 on migration of endothelial cells, HUVECs were cultured on the gelatin-coated dishes at 90% confluence and wounded with a blade. The degree of migration was quantified by counting the cells that migrated beyond the reference line in randomly selected fields (original magnification ×200). rhLK8 suppressed migration of endothelial cells stimulated by VEGF. Each experiment was repeated at least three times, and the data are presented as mean ± SD. *$P < 0.05$ (compared to control). **$P < 0.05$ (compared to VEGF treatment).
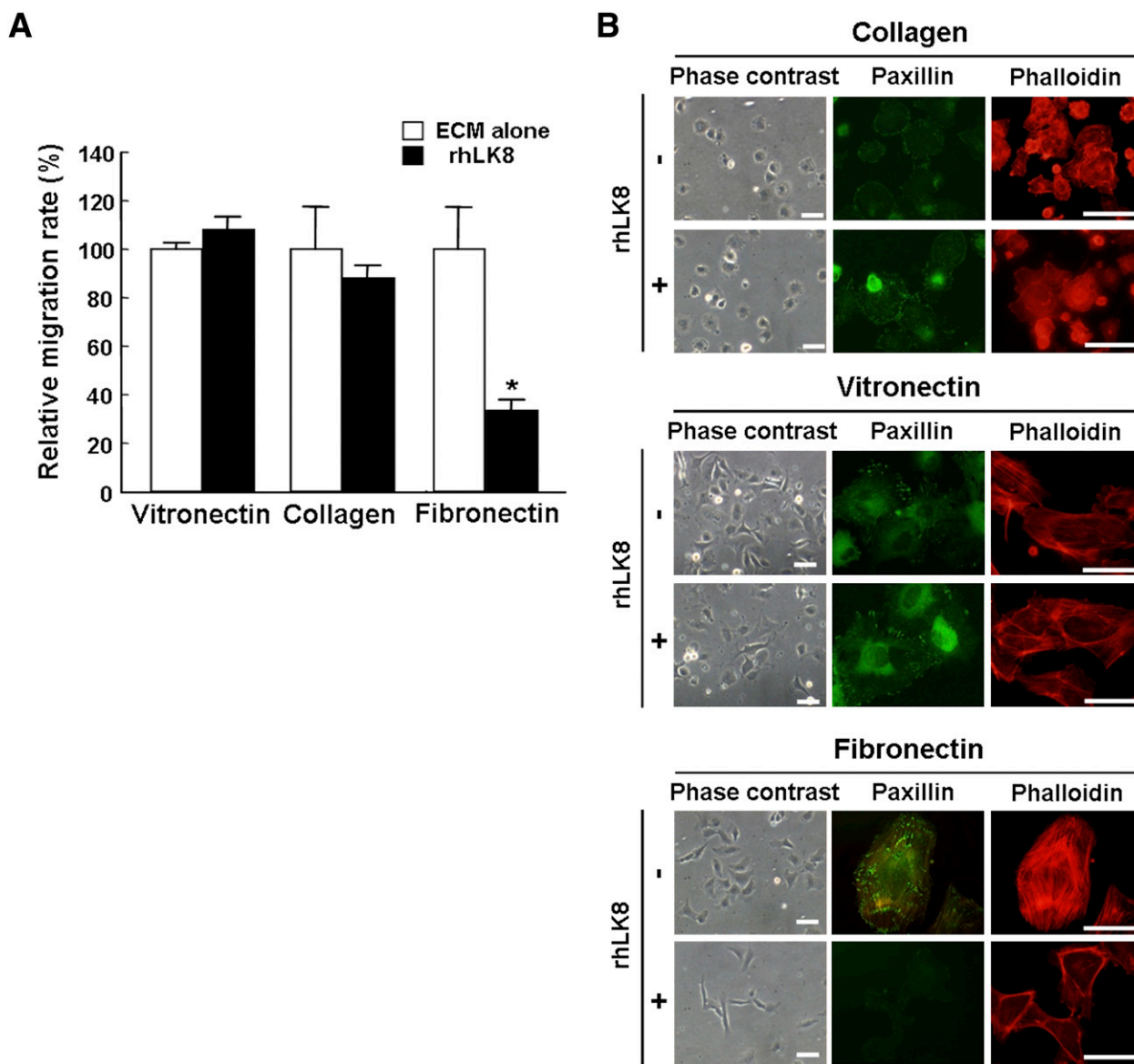
A

B

FIG. 3. rhLK8 suppresses migration of endothelial cells on FN, and FN-stimulated formation of actin filaments and focal adhesion complexes. *A*: Boyden chambers were precoated with VN, collagen, or FN for 2 h at RT. Suspended endothelial cells were treated with or without rhLK8, added to each Boyden chamber, and incubated for 4 h at 37°C. After the incubation, cells were fixed and stained with crystal violet. The degree of migration was assessed by measuring the absorbance of eluted dye solution at 595 nm. Data are expressed as percentage compared with controls. *B*: Cell adhesion assay showed that endothelial cells plated on FN exhibited smaller and less organized morphology when treated with rhLK8. However, rhLK8 did not affect the adhesiveness of the cells incubated on VN or collagen. Formation of actin stress fibers and focal adhesion complexes was also assessed by immunofluorescent staining with antibody against phalloidin and paxillin. Interestingly, rhLK8 only affected FN-mediated formation of actin filaments and focal adhesion complexes. Scale bar, 50 μm. (A high-quality digital representation of this figure is available in the online issue.)

images showed that HUVECs plated on FN exhibited smaller and less organized morphology when treated with rhLK8. When cells were placed on other ECM proteins, rhLK8 did not affect cellular morphology and adhesiveness (Fig. 3*B*).

We previously demonstrated the inhibitory effect of rhLK8 on the formation of actin stress fibers, as demonstrated by phalloidin staining, and on focal adhesions, as demonstrated by paxillin staining (10). In this study, rhLK8 inhibited the formation of actin filaments and focal adhesions complexes when endothelial cells were placed on FN (Fig. 3*B*). When the cells were placed on collagen or VN, rhLK8 did not exert any change in cellular structure and formation of focal adhesions.

Inhibition of migration on FN by rhLK8 is related with suppression of α3β1 integrin. From the results of migration and cell adhesion assays, integrin was supposed to be the target of rhLK8. The integrins known to be expressed on endothelial cells include α1β1, α2β1, α3β1, α4β1, α5β1, α6β1, α6β4, α9β1, αvβ1, αvβ3, αvβ5, and αvβ8 integrin (22–24). Because rhLK8 only inhibited cell migration associated with FN, we could focus on integrin subunits that had the FN ligand: integrin αv, α3, α5, β1, and β3 (25). As shown in Fig. 4*A*, flow cytometric analysis demonstrated that HUVECs expressed more β1 integrin than β3 integrin. The expressions of the αv, α3, and α5 integrin subunits were similar.

To identify subtypes of integrin to which rhLK8 bound, we treated HUVECs with monoclonal antibodies against
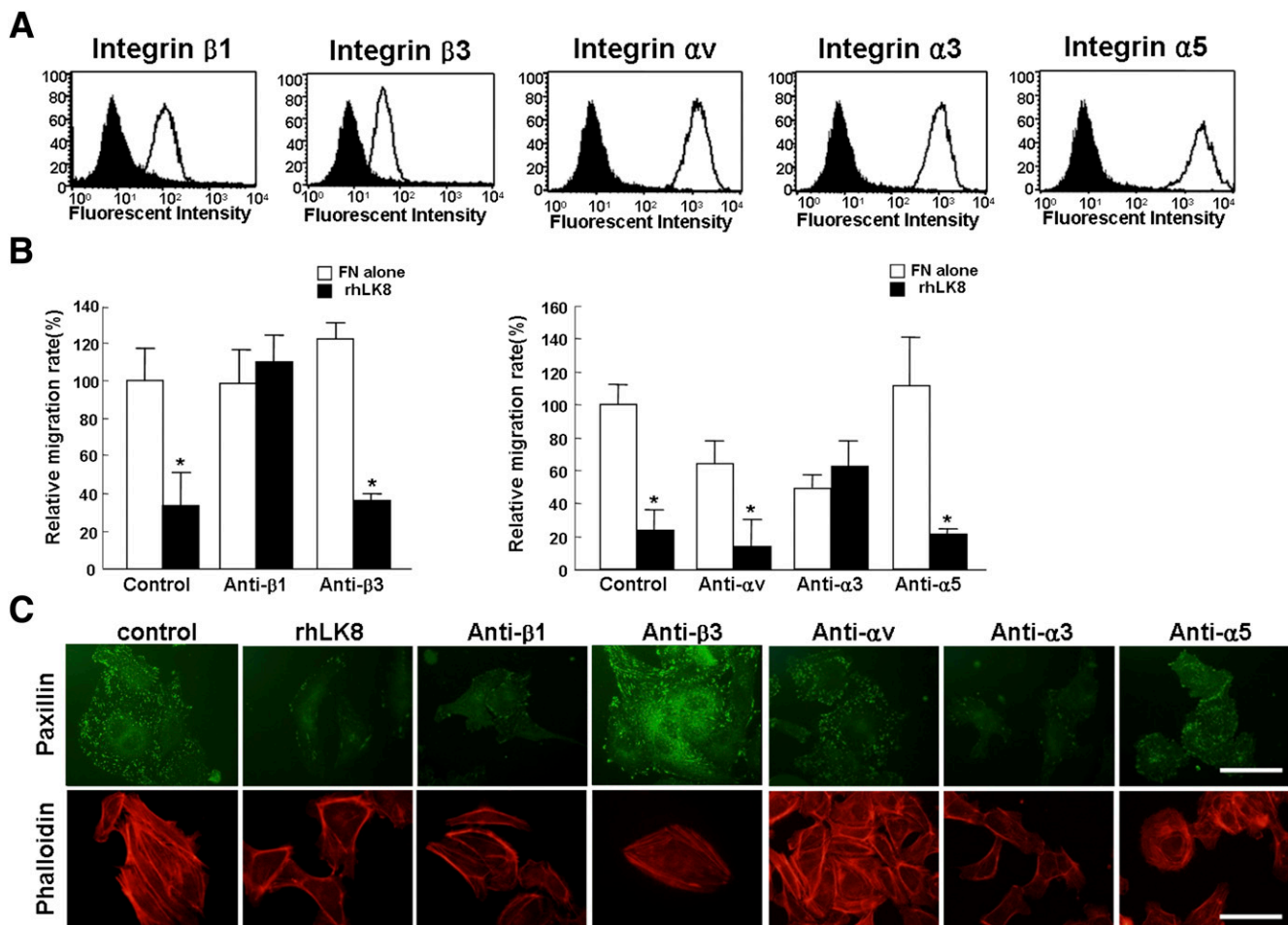
FIG. 4. Effects of rhLK8 and antibodies against integrin subunits on migration of endothelial cells and formation of actin stress fibers and focal adhesions. *A*: Flow cytometric analyses demonstrated differential expression of integrin subunits on HUVECs. We chose for the analysis integrin subunits of which the ligand was FN, αv, α3, α5, β1, and β3 integrins because rhLK8 inhibited FN-mediated angiogenesis from earlier experiments. *B*: HUVECs were treated with monoclonal antibodies against specific α and β subunits of integrin (0.5 μg/mL) or rhLK8 and were allowed to migrate on FN for 4 h. Experiments were performed at least three times, and data are presented as mean ± SD compared with controls. *P < 0.05. *C*: Suspended HUVECs treated with 0.5% BSA, rhLK8 (1 μmol/L), or monoclonal antibodies against integrin subunits for 30 min were inoculated on the 6-well plates coated with FN. Effects of rhLK8 and antibodies against integrin subunits on formation of focal adhesions and actin filaments were evaluated with immunofluorescence staining. Scale bar, 50 μm. (A high-quality digital representation of this figure is available in the online issue.)

each subunit of integrin and assessed the inhibitory effect of rhLK8 on migration. When cells were pretreated with antibodies to integrin β1 or α3, rhLK8 did not exert additive inhibition on the migration of endothelial cells. However, when integrins β3, αv, or α5 were suppressed with monoclonal antibodies, rhLK8 showed similar inhibitory effects (Fig. 4*B*). In addition, we performed immunofluorescent staining for paxillin and phalloidin in cells plated on FN with the treatment of rhLK8 or monoclonal antibodies against subunits of integrin. Immunoreactivity for paxillin and phalloidin was decreased in cells treated with rhLK8 or monoclonal antibodies to β1 or α3 integrin, demonstrating that those treatments affected the formation of actin filaments and focal adhesions (Fig. 4*C*).

We performed protein microarray for observation of direct interactions between rhLK8 and presumed target integrins αvβ3, α1β1, α3β1, and α5β1. We chose α3β1 and α5β1 integrin, because integrin β1 showed higher expression in endothelial cells than integrin β3, and the three α subunits showed similar expression patterns in the flow cytometry. We omitted αvβ1 integrin from the list because this integrin is not expressed much in endothelial cells.

Instead, αvβ3 and α1β1 integrins were included because they are abundant in endothelial cells. The protein microarray showed that the interaction between α3β1 integrin and rhLK8 was the most intensive compared with interactions between other integrins and rhLK8 (Fig. 5*A*). The binding intensity between rhLK8 and α3β1 integrin was equivocal with that between rhLK8 and monoclonal antibody against rhLK8 when rhLK8 was 1 μmol/L (Fig. 5*B*).

Then, we downregulated transcription of integrin β1 or β3 with siRNA and assessed the effect of rhLK8 on migration. As expected from previous experiments, rhLK8 did not exert an additional effect when cells were treated with siRNA for integrin β1 but showed inhibitory effect when cells were treated with siRNA for integrin β3. The treatment with siRNA for integrin β1 suppressed migration of endothelial cells (Fig. 6*A*).

We also performed immunoprecipitation and immunoblotting to show direct interaction between integrin β1 and rhLK8. As shown in Fig. 6*B*, immune complexes of integrin β1 and rhLK8 were evident. Immunofluorescent staining showed that integrin β1 and rhLK8 were merged at the edge of the endothelial cells (Fig. 6*C*).
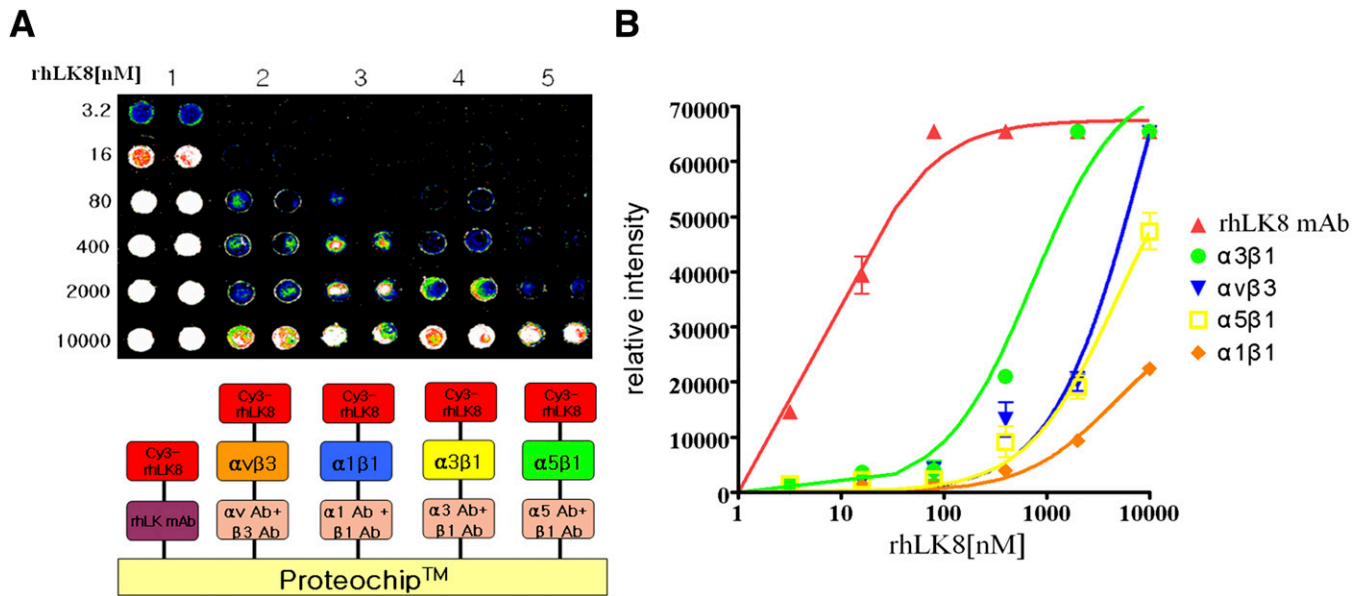
FIG. 5. Detection of the protein–protein interaction between specific subtypes of integrin and rhLK8. *A*: A mixture of monoclonal antibodies to α and β subunits of integrin was immobilized on the ProLinker-coated microarray spot surface; then, integrin subunits (αvβ3, α1β1, α3β1, and α5β1 integrins) were immobilized on the antibodies against integrin subunits for 1 h at RT. The microarray was incubated with Cy3-labeled rhLK8 at concentrations from 3.2 nmol/L to 10 μmol/L for 1 h at 23°C. The microarray was scanned using a fluorescence scanner. *B*: Relative intensity curve showed the intensity of protein-protein interaction between subtypes of integrin and rhLK8. (A high-quality digital representation of this figure is available in the online issue.)

rhLK8 inhibited phosphorylation of FAK, resulting in suppression of JNK activation. As we previously reported, rhLK8 did not affect phosphorylation of ERK1/2, but reduced activation of FAK, demonstrating a distinctive feature from rhLK68, which consisted of kringle domain IV-9, IV-10, and V, suppressing phosphorylation of ERK1/2 (10,11). We further investigated phosphorylation, of which tyrosine residue of FAK was suppressed by rhLK8. Interestingly, rhLK8 suppressed phosphorylation of FAK at Tyr397, activated by adhesion on FN; however, rhLK8
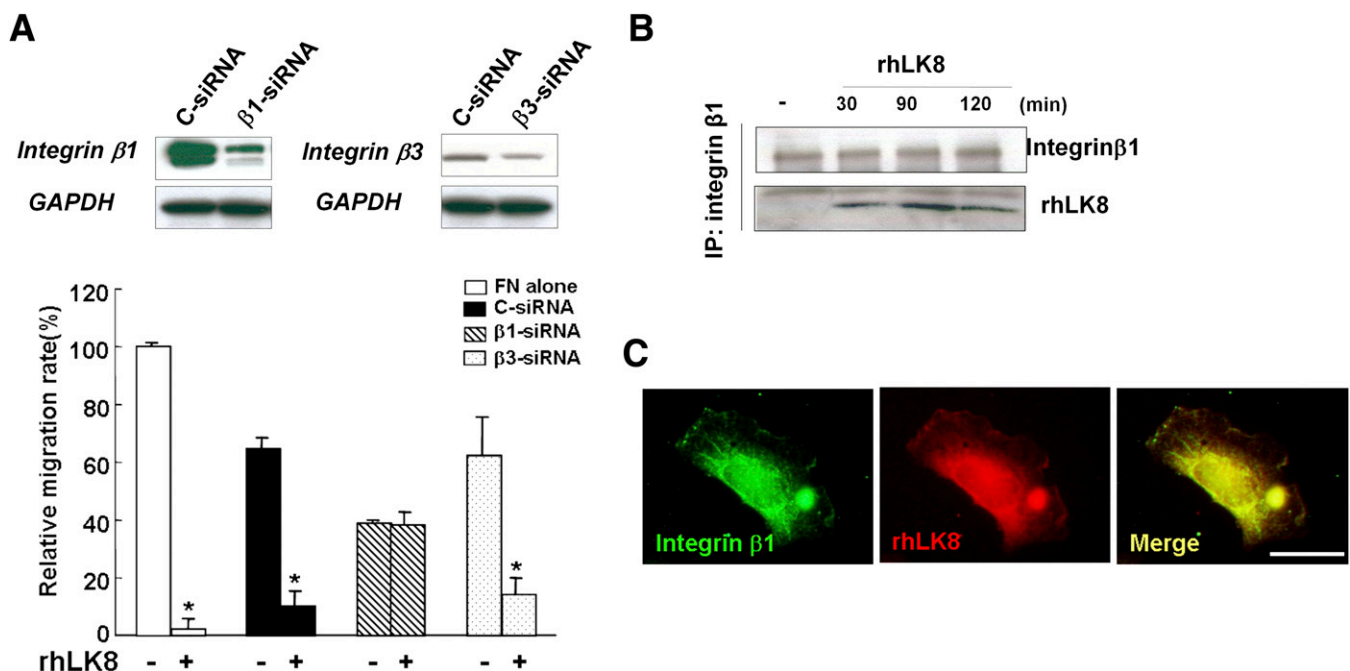

FIG. 6. The inhibitory effect of rhLK8 on migration of endothelial cells is related with suppression of integrin β1. *A*: We downregulated transcription of integrin β1 or β3 with siRNA and assessed the additional effect of rhLK8 on migration of endothelial cells. Data are expressed as percentage of control values (set to 100). Values ± SD are from three independent experiments. GAPDH, glyceraldehyde-3-phosphate dehydrogenase.*$P < 0.05$. *B*: HUVECs were treated with rhLK8 and plated on FN for 90 min. Cells were lysed and immunoprecipitated with antibodies against integrin β1. The immunocomplexes were resolved by SDS-PAGE and analyzed by immunoblotting using the antibody against rhLK8. *C*: HUVECs were treated with rhLK8 and plated on FN-coated coverslips for 90 min. Cells were fixed and stained with antibodies to integrin β1 and rhLK8. (A high-quality digital representation of this figure is available in the online issue.)

did not change phosphorylation of other tyrosine resides (Fig. 7A). We also confirmed previous data that rhLK8 did not affect phosphorylation of ERK1/2 (Fig. 7B) and continued experiments on downstream targets of integrin-FAK signaling pathways. The interaction between p130CAS and phosphorylated FAK was identified in the immunoprecipitation assay (Fig. 7C). Further experiments showed decreased

phosphorylation of JNK by rhLK8, demonstrating that rhLK8 might exert its action via suppressing FAK-p130CAS–mediated JNK activation.

In addition, to confirm the inhibitory effect of rhLK8 on activation of JNK but not ERK or phosphatidylinositol-3-kinase (PI3K), we assessed the change of migration according to the treatment with rhLK8 or JNK, PI3K, and ERK
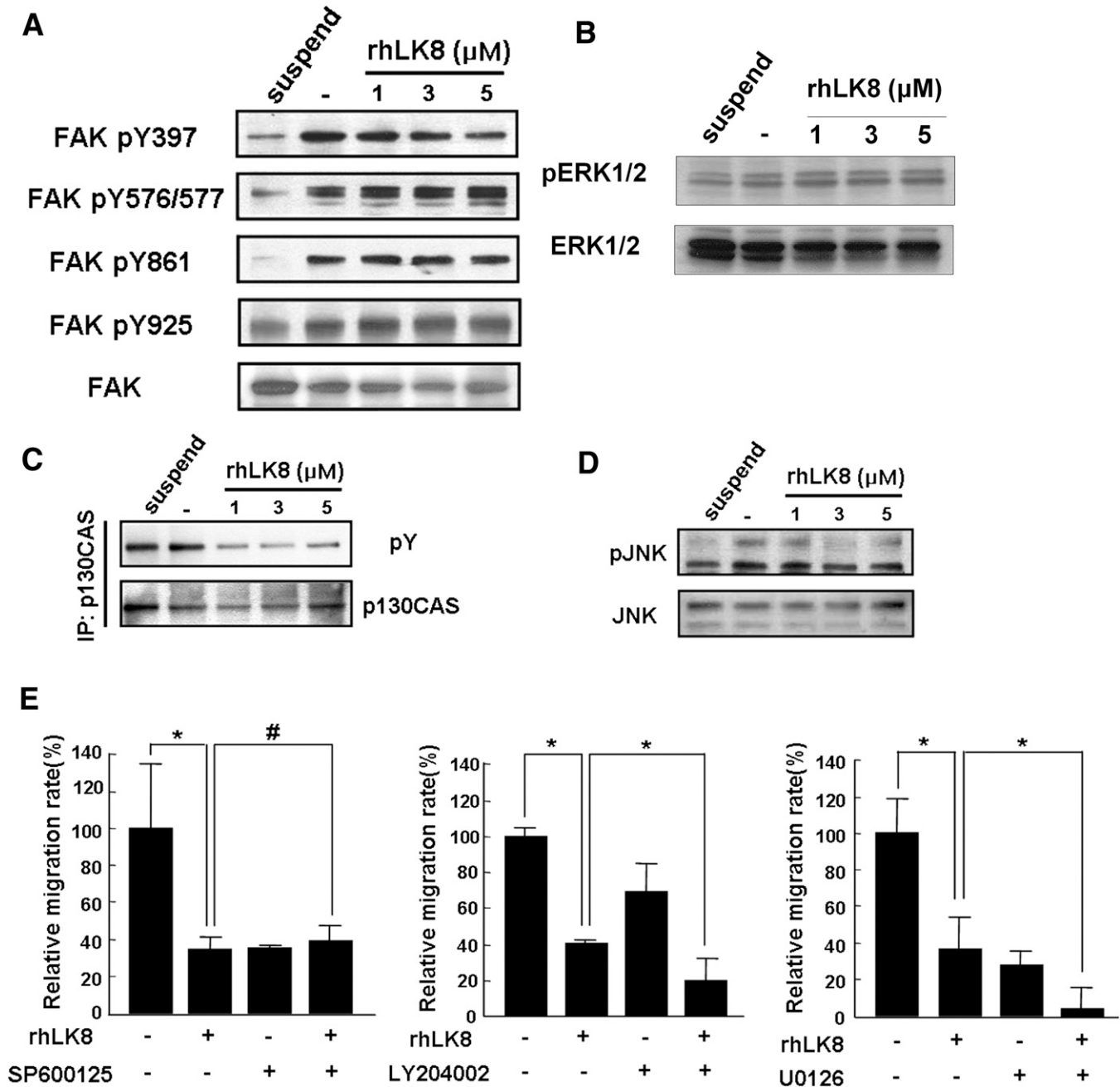

FIG. 7. rhLK8 inhibits phosphorylation of FAK at Tyr397, resulting in suppression of activation of p130CAS–JNK pathway. A: HUVECs were treated with different concentrations of rhLK8, placed onto FN-coated plates for 90 min, and lysed. Phosphorylation of Tyr397, Tyr576/577, Tyr861, and Tyr925 of FAK was increased on adhesion with FN; however, with the treatment of rhLK8, only phosphorylation of Tyr397 of FAK was inhibited in a dose-dependent manner. B: Adhesion of endothelial cells with FN did not affect phosphorylation of ERK1/2, neither did rhLK8 inhibit phosphorylation of ERK1/2. C: HUVECs were treated with different concentrations of rhLK8 and plated on FN for 90 min. Cells were lysed and immunoprecipitated with antibodies against p130CAS. The immunocomplexes were resolved by SDS-PAGE and analyzed by immunoblotting using the antibody against phosphorylated FAK. D: Adhesion of endothelial cells with FN induced phosphorylation of JNK, which was inhibited by rhLK8. E: HUVECs were treated with SP600125, LY294002, and U0126 for 10 min, followed by rhLK8 for 30 min, and were allowed to migrate on FN for 4 h. Values are expressed as percentage of the control value (set to 100). Values ± SD are from three independent experiments. *$P < 0.05$. #$P > 0.05$.

inhibitors (SP600125, LY204002, and U0126, respectively). As expected, rhLK8 did not show an additive effect on migration when cells were pretreated with JNK inhibitor.

DISCUSSION

In this study, we demonstrated that rhLK8 inhibited retinal neovascularization, emphasizing possible application of rhLK8 in the treatment of FN-associated pathologic angiogenesis. We previously reported that rhLK8 exerted an antiangiogenic effect and that the recombinant adeno-associated virus–carrying gene encoding kringle domain V suppressed the growth of hepatocellular carcinoma in mice via inhibition of tumor angiogenesis (10,26). In this study, rhLK8 also effectively inhibited tube formation and migration of HUVECs in a dose-dependent manner at the concentrations administered without definite cellular and retinal toxicities.

DR is characterized by retinal neovascularization from inner layers of the retina (1,3). In particular, complications of retinal neovascularization in DR come from the proliferation of retinal neovessels into the vitreous cavity. Vitreous is composed of various ECM proteins and a network of glycosaminoglycans that fills the spaces between proteins and helps to maintain vitreous volume (27). Of the ECM proteins, collagen takes up most of the portions, and FN is second in quantity (4). Interestingly, in patients with DR, FN was elevated in vitreous, plasma, and newly formed capillaries or retinal microvessels (5–8,28). FN binds to integrin receptors and converts to an active form, promoting FN-fibril formation outside of the cells (29). Furthermore, FN was known to activate angiogenesis, and a specific spliced form of FN was involved in endothelial cell proliferation and vascular morphogenesis (30). In DR, this form of FN was overexpressed in vitreous cavity (6,30).

In this study, we observed that rhLK8 inhibited migration of HUVECs via the Boyden chamber coated with FN but exerted no effect on migration associated with VN and collagen. Phase-contrast images showed that endothelial cells on FN were smaller and less organized when treated with rhLK8. Furthermore, we assessed the formation of actin stress fibers and activation of focal adhesion complexes. Paxillin, a FAK-binding protein, is recruited on adhesion of ECM proteins with integrin (31). By interacting with talin and paxillin, FAK localizes to the sites of integrin clustering, initiating downstream signaling pathways in relation with cell migration, invasion, or adhesion (32,33). Interestingly, rhLK8 suppressed formation of actin filaments and activation of focal adhesion complexes by FN. From these results, we formulated a small hypothesis that integrin, which had affinity to FN, might be involved in the action of rhLK8.

Integrins that have been known to be involved in angiogenesis and expressed in endothelial cells include α1β1, α2β1, α3β1, α4β1, α5β1, α6β1, α6β4, α9β1, αvβ1, αvβ3, αvβ5, and αvβ8 integrins (22–24). Integrins, heterodimeric membrane glycoproteins composed of α and β subunits, promote cell attachment and migration on ECM (22). For these functions, each subunit of integrin recognizes specific ECM proteins as ligands (34). In our study, rhLK8 inhibited cell migration associated with FN only; therefore, we focused on integrins with the FN ligand: integrins αv, α3, α5, β1, and β3 (25). To determine the effect of the integrin subtypes on the action of rhLK8, we downregulated each integrin subtype and assessed the additional effect of rhLK8

on cell migration. Interestingly, when cells were treated with monoclonal antibodies against integrin α3 and β1, we could not observe any additional effect of rhLK8 on cell migration. In addition, the treatment with monoclonal antibodies against integrin α3 and β1 resulted in a decrease in the formation of actin filaments and focal adhesion complex because rhLK8 inhibited them. From these results, integrin α3 and β1 were regarded as presumed targets of rhLK8.

The protein microarray showed the binding intensity between rhLK8 and α3β1 integrin was similar to that between rhLK8 and monoclonal antibody against rhLK8 at the concentration of 1 μmol/L. Immunoprecipitation with integrin β1 and immunoblotting with rhLK8 also demonstrated binding between rhLK8 and β1 integrin. In endothelial cells treated with rhLK8, immunofluorescent staining for integrin β1 and rhLK8 were merged at the edge of the endothelial cells. α3β1 integrin is implicated in various biologic phenomena, including establishment and maintenance of epithelial tissues, cell growth, apoptosis, and angiogenesis (35). This integrin forms a large complex with various membrane proteins such as the transmembrane-4 superfamily proteins, cytoskeletal proteins, and intracellular signaling molecules. In addition, α3β1 integrin binds to ECM-bound VEGF, promoting adhesion, migration, and cellular survival of endothelial cells (23). VEGF was increased in the vitreous in DR, and this was implicated in the progression of DR (36). The inhibitory effect of rhLK8 on FN-associated angiogenesis might be partially caused by inhibition of α3β1 integrin from forming functioning complexes with VEGF.

We previously reported that rhLK8 inhibited FGF-stimulated phosphorylation of FAK (10). In this study, we performed further experiments on signaling pathways regarding the action of rhLK8. FAK is phosphorylated at Tyr397 when it binds to the intracellular domain of integrins, promoting phosphorylation of Tyr576/577 in the kinase domain activation loop, and Tyr861 or Tyr925 in the COOH-terminal domain (37,38). FAK was phosphorylated at all tyrosine residues when endothelial cells were cultured on FN-coated plates. Interestingly, the treatment with rhLK8 affected the phosphorylation of FAK at Tyr397; however, no change occurred in phosphorylation of FAK at the other residues. By inactivation of FAK at Tyr397, rhLK8 might influence downstream signaling molecules of the FAK-related signaling pathway. Because we found that there was no change in phosphorylation of ERK1/2, which was activated by phosphorylation of FAK at Tyr925 (39), we focused on another downstream signaling cascade, the p130CAS–JNK pathway. Interestingly, immunoprecipitation showed ligation between phosphorylated FAK and p130CAS. In addition, rhLK8 inhibited phosphorylation of JNK, and when cells were treated with the JNK inhibitor SP600125, rhLK8 did not exert additional effect on cell migration, demonstrating JNK inhibition was a plausible mechanism of the action of rhLK8.

In summary, rhLK8 has an antiangiogenic effect on retinal neovascularization. In vitro studies suggest that rhLK8 may inhibit angiogenesis by disrupting FN-mediated migration of endothelial cells. rhLK8 may interfere with the interaction between α3β1 integrin and ECM, suppressing the FAK–p130CAS–JNK pathway. We suggest that rhLK8 could possibly be applied in the treatment of matrix-mediated pathologic angiogenesis, including retinal neovascularization in DR.

REFERENCES

1. Jo DH, Kim JH, Kim JH. How to overcome retinal neuropathy: the fight against angiogenesis-related blindness. Arch Pharm Res 2010;33:1557–1565
2. Penn JS, Madan A, Caldwell RB, Bartoli M, Caldwell RW, Hartnett ME. Vascular endothelial growth factor in eye disease. Prog Retin Eye Res 2008;27:331–371
3. Frank RN. Diabetic retinopathy. N Engl J Med 2004;350:48–58
4. Badylak SF. The extracellular matrix as a scaffold for tissue reconstruction. Semin Cell Dev Biol 2002;13:377–383
5. Casaroli Marano RP, Preissner KT, Vilaró S. Fibronectin, laminin, vitronectin and their receptors at newly-formed capillaries in proliferative diabetic retinopathy. Exp Eye Res 1995;60:5–17
6. George B, Chen S, Chaudhary V, Gonder J, Chakrabarti S. Extracellular matrix proteins in epiretinal membranes and in diabetic retinopathy. Curr Eye Res 2009;34:134–144
7. Probst K, Fijnheer R, Schellekens P, Rothova A. Intraocular and plasma levels of cellular fibronectin in patients with uveitis and diabetes mellitus. Br J Ophthalmol 2004;88:667–672
8. Roy S, Cagliero E, Lorenzi M. Fibronectin overexpression in retinal microvessels of patients with diabetes. Invest Ophthalmol Vis Sci 1996;37:258–266
9. Cherian S, Roy S, Pinheiro A, Roy S. Tight glycemic control regulates fibronectin expression and basement membrane thickening in retinal and glomerular capillaries of diabetic rats. Invest Ophthalmol Vis Sci 2009;50:943–949
10. Kim JS, Yu HK, Ahn JH, et al. Human apolipoprotein(a) kringle V inhibits angiogenesis in vitro and in vivo by interfering with the activation of focal adhesion kinases. Biochem Biophys Res Commun 2004;313:534–540
11. Kim JS, Chang JH, Yu HK, et al. Inhibition of angiogenesis and angiogenesis-dependent tumor growth by the cryptic kringle fragments of human apolipoprotein(a). J Biol Chem 2003;278:29000–29008
12. Cao Y, Cao R, Veitonmäki N. Kringle structures and antiangiogenesis. Curr Med Chem Anticancer Agents 2002;2:667–681
13. Kim JH, Kim JH, Yu YS, Kim DH, Kim CJ, Kim KW. Establishment and characterization of a novel, spontaneously immortalized retinoblastoma cell line with adherent growth. Int J Oncol 2007;31:585–592
14. Lee TH, Kim MD, Shin SY, Lim HK, Seo JH. Disruption of hexokinase II (HXK2) partly relieves glucose repression to enhance production of human kringle fragment in gratuitous recombinant Saccharomyces cerevisiae. J Biotechnol 2006;126:562–567
15. Kang KY, Park JH, Lim IH, et al. Crystallization of antiangiogenic Kringle V derived from human apolipoprotein A: crystallization applied to purification and formulation. Biosci Biotechnol Biochem 2006;70:916–925
16. Kim JH, Kim JH, Yu YS, Shin JY, Lee HY, Kim KW. Deguelin inhibits retinal neovascularization by down-regulation of HIF-1alpha in oxygen-induced retinopathy. J Cell Mol Med 2008;12:2407–2415
17. Smith LE, Wesolowski E, McLellan A, et al. Oxygen-induced retinopathy in the mouse. Invest Ophthalmol Vis Sci 1994;35:101–111
18. Min JK, Cho YL, Choi JH, et al. Receptor activator of nuclear factor (NF)-kappaB ligand (RANKL) increases vascular permeability: impaired permeability and angiogenesis in eNOS-deficient mice. Blood 2007;109:1495–1502
19. Kim JH, Kim JH, Yu YS, et al. Antiangiogenic effect of deguelin on choroidal neovascularization. J Pharmacol Exp Ther 2008;324:643–647
20. Lee Y, Lee EK, Cho YW, et al. ProteoChip: a highly sensitive protein microarray prepared by a novel method of protein immobilization for application of protein-protein interaction studies. Proteomics 2003;3:2289–2304
21. Ausprunk DH, Folkman J. Migration and proliferation of endothelial cells in preformed and newly formed blood vessels during tumor angiogenesis. Microvasc Res 1977;14:53–65
22. Avraamides CJ, Garmy-Susini B, Varner JA. Integrins in angiogenesis and lymphangiogenesis. Nat Rev Cancer 2008;8:604–617
23. Hutchings H, Ortega N, Plouët J. Extracellular matrix-bound vascular endothelial growth factor promotes endothelial cell adhesion, migration, and survival through integrin ligation. FASEB J 2003;17:1520–1522
24. Hynes RO. Cell-matrix adhesion in vascular development. J Thromb Haemost 2007;5(Suppl. 1):32–40
25. Silva R, D'Amico G, Hodivala-Dilke KM, Reynolds LE. Integrins: the keys to unlocking angiogenesis. Arterioscler Thromb Vasc Biol 2008;28:1703–1713
26. Lee K, Yun ST, Kim YG, Yoon Y, Jo EC. Adeno-associated virus-mediated expression of apolipoprotein (a) kringles suppresses hepatocellular carcinoma growth in mice. Hepatology 2006;43:1063–1073
27. Bishop PN. Vitreous as a substrate for vitreolysis. Dev Ophthalmol 2009;44:7–19
28. Seghieri G, Bartolomei G, De Giorgio LA. Plasma fibronectin in diabetic retinopathy and macroangiopathy. Diabete Metab 1986;12:186–190
29. Wierzbicka-Patynowski I, Schwarzbauer JE. The ins and outs of fibronectin matrix assembly. J Cell Sci 2003;116:3269–3276
30. Khan ZA, Chan BM, Uniyal S, et al. EDB fibronectin and angiogenesis—a novel mechanistic pathway. Angiogenesis 2005;8:183–196
31. Deakin NO, Turner CE. Paxillin comes of age. J Cell Sci 2008;121:2435–2444
32. Arold ST, Hoellerer MK, Noble ME. The structural basis of localization and signaling by the focal adhesion targeting domain. Structure 2002;10:319–327
33. Harburger DS, Calderwood DA. Integrin signalling at a glance. J Cell Sci 2009;122:159–163
34. Plow EF, Haas TA, Zhang L, Loftus J, Smith JW. Ligand binding to integrins. J Biol Chem 2000;275:21785–21788
35. Tsuji T. Physiological and pathological roles of alpha3beta1 integrin. J Membr Biol 2004;200:115–132
36. Aiello LP, Avery RL, Arrigg PG, et al. Vascular endothelial growth factor in ocular fluid of patients with diabetic retinopathy and other retinal disorders. N Engl J Med 1994;331:1480–1487
37. Schwartz MA. Integrin signaling revisited. Trends Cell Biol 2001;11:466–470
38. Van Slambrouck S, Grijelmo C, De Wever O, et al. Activation of the FAK-src molecular scaffolds and p130Cas-JNK signaling cascades by alpha1-integrins during colon cancer cell invasion. Int J Oncol 2007;31:1501–1508
39. Schlaepfer DD, Jones KC, Hunter T. Multiple Grb2-mediated integrin-stimulated signaling pathways to ERK2/mitogen-activated protein kinase: summation of both c-Src- and focal adhesion kinase-initiated tyrosine phosphorylation events. Mol Cell Biol 1998;18:2571–2585